Impact of the homogeneous junction breakdown in IBC solar cells on the passivation quality of Al 2 O 3 and SiO 2 : degradation and regeneration behavior

Available online at www.sciencedirect.com

ScienceDirect

Energy Procedia 124 (2017) 365–370

Energy Procedia

www.elsevier.com/locate/procedia

7th International Conference on Silicon Photovoltaics, SiliconPV 2017

Impact of the homogeneous junction breakdown in IBC solar cells on the passivation quality of Al_2O_3 and SiO_2: degradation and regeneration behavior

Ralph Müller[a,b,*], Christian Reichel[a], Xinbo Yang[c,d], Armin Richter[a], Jan Benick[a], Martin Hermle[a]

[a]*Fraunhofer Institute for Solar Energy Systems (ISE), Heidenhofstraße 2, D-79110 Freiburg, Germany*
[b]*Albert Ludwig University Freiburg, Department of Sustainable Systems Engineering, Georges-Köhler-Allee 103, D-79110 Freiburg, Germany*
[c]*Research School of Engineering, Australian National University, Canberra, ACT 2601, Australia*
[d]*Solar Center, Division of Physical Sciences and Engineering, King Abdullah University of Science and Technology, Thuwal 23955-6900, Kingdom of Saudi Arabia*

Abstract

Within the last years, many different approaches for the simplified fabrication of interdigitated back-contact (IBC) solar cells have been developed. Most of those concepts result in emitter and back-surface field (BSF) regions that are in direct contact to each other which leads to a controlled breakdown under reverse bias at the p^+n^+ junction. In this work, the influence of the reverse breakdown on the passivation quality of Al_2O_3 and SiO_2 at the p^+n^+ junction is investigated, not only shedding light on the degradation but also on the regeneration behavior of the cells. It was found that cells with Al_2O_3 passivation on the back side degrade during reverse breakdown whereas sister cells with SiO_2 passivation were rather unaffected. Consequently, the degradation seems to be related to the passivation layer. However, it is shown that the passivation can be regenerated even under normal operation condition. A possible explanation is the discharging of interface traps, which are getting recharged already at room temperature.

Peer review by the scientific conference committee of SiliconPV 2017 under responsibility of PSE AG.

Keywords: Silicon; Solar cell; Back Contact; Back junction; Reverse bias; Breakdown; Passivation

* Corresponding author. Tel.: +49-761-4588-5921; fax: +49-761-4588-9250.
E-mail address: ralph.mueller@ise.fraunhofer.de

1876-6102
Peer review by the scientific conference committee of SiliconPV 2017 under responsibility of PSE AG.
10.1016/j.egypro.2017.09.311

1. Introduction

Interdigitated back-contact (IBC) solar cells have a very high efficiency potential [1, 2] but typically come along with a complex fabrication process. Several approaches for simplifications of the process flow have been suggested within the last years [3-11]. The simplifications are often based on self-aligning processes, i.e. the masking of one dopant type (or source) by the other dopant type (or source) [3, 7-10]. This inherently leads to a steep doping gradient at the transition from emitter to back-surface field (BSF) with very thin space charge regions on both sides of this p^+n^+ junction. Consequently, the junction shows a breakdown at low voltage when reverse biased [3, 4, 12].

SunPower has proven that their IBC solar cells show a non-damaging reverse breakdown that is even beneficial for the module performance compared to standard cell concepts when a part of the module is shadowed [13]. On the other hand, it was found that the reverse breakdown can affect the cell performance even if it occurs homogeneously along the whole p^+n^+ junction in a controlled way [12], but the reason is still unknown.

In this work, a direct comparison of identically processed IBC solar cells with either Al_2O_3 or SiO_2 passivation on the back side (see Fig. 1) is made in order to test the influence of the passivation layer on the solar cell degradation under reverse bias. Additionally, the regeneration at different temperature regimes over time is investigated.

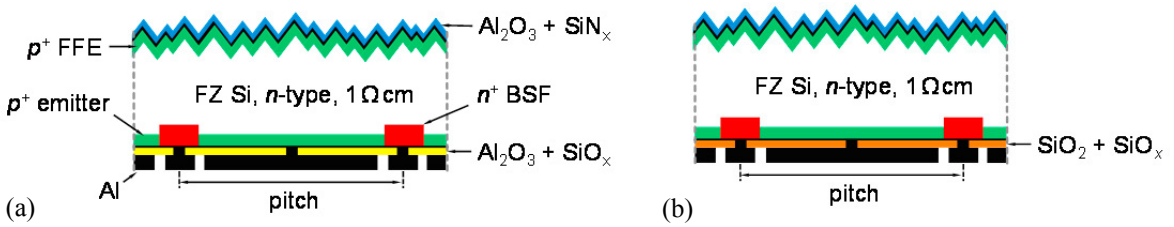

Fig. 1. Schematic of the IBC solar cells with BSF formed by local ion implantation of phosphorus and subsequent BBr_3 furnace diffusion to form the emitter and anneal the phosphorus implantation [7]. The pitch is 0.5 mm with 0.4 mm emitter width and 0.1 mm BSF width. The cells were processed identically, but the thermally grown SiO_2 was either kept as back-side passivation layer and capped with SiO_x (b) or replaced by an Al_2O_3 / SiO_x stack (a). (FFE = front floating emitter)

2. Experimental

Solar cells were fabricated on 1 Ω cm n-type FZ silicon wafers with 200 µm thickness. The samples were textured on the front side with KOH forming random pyramids. Phosphorus was implanted locally on the back side (3×10^{15} cm^{-2}, 10 keV) to form the BSF. All the masking in the fabrication was done by a photoresist. Emitter and front floating emitter (FFE) were realized by a full-area BBr_3 furnace diffusion (890 °C, 1 h). After removing the boron glass, a ~40 nm thick oxide was grown in a tube furnace at the Australian National University. The thermal oxide was either kept as back-side passivation layer (see Fig. 1b) or removed in HF and replaced by a 10 nm thick Al_2O_3 layer (plasma-assisted atomic layer deposition, PA-ALD). The back side (passivated with either Al_2O_3 or SiO_2) was then capped with 100 nm SiO_x (plasma-enhanced chemical vapour deposition, PECVD) (see Fig. 1a). On the front side, the Al_2O_3 was capped with 60 nm SiN_x (PECVD). Before metallization, all samples received a forming gas anneal at 425 °C for 25 min to activate the Al_2O_3 passivation. Contact openings on the back side were etched in HF, Al was evaporated and wet-chemically structured. Finally, the finished cells were tempered at 300 °C for 5 min on a hotplate to improve the metal contact.

3. Results

3.1. IBC solar cells

The cell parameters of the best solar cells from both groups (either Al_2O_3 or SiO_2 back-side passivation) are summarized in Table 1. The thermally grown SiO_2 offers a very good surface passivation for the ~160 Ω/sq boron emitter with a recombination current density prefactor (J_0) of only 13 fA/cm^2 on a planar surface (compared to

9 fA/cm^2 for Al_2O_3). Hence, the open-circuit voltage (V_{OC}) of 674 mV is at a similar level as the Al_2O_3 passivated cells (671 mV). For both cells, the V_{OC} is limited by recombination in the highly-doped BSF region. The deviation in short-circuit current density (J_{SC}) are related to slight differences in the front reflection (texture and SiN_x anti-reflection coating). The fill factor (*FF*) of all cells is well above 81 % due to the small pitch and low series resistance and the energy conversion effieciency (η) is above 22 %.

Table 1. Solar cell parameters of the best cells measured under standard testing conditions (25 °C, AM1.5G, 1000 W/cm^2). The pseudo fill factor (*pFF*) was measured by SunsVoc.

Aperture cell area: 4 cm^2 (best cell results)	V_{oc} [mV]	J_{sc} [mA/cm^2]	*FF* [%]	*pFF* [%]	η [%]
Back-side passivation: Al_2O_3	671	40.5	81.4	82.4	22.1
Back-side passivation: SiO_2	674	40.9	81.6	82.9	22.5

3.2. Junction breakdown in reverse-biased cells

The IBC solar cells show a controlled junction breakdown at low voltage, which occurs homogeneously distributed along the whole p^+n^+ junction [12]. At a reverse bias of -6.7 V, the current density is in the range of J_{SC} (~40 mA/cm^2) for both types of back-side passivation. These conditions are representative for a shadowed solar cell in a string with all other cells illuminated, because the illuminated cells force a current flow through the shadowed cell. The influence of the reverse breakdown on the solar cell parameters was investigated by alternately switching from current-voltage (IV) measurement to reverse bias.

Fig. 2 shows a comparison of two IBC solar cells with different back-side passivation layers. Initially, the V_{OC} was very similar (~665 mV) and high fill factors of ~82 % were observed for both cells. Each time after reverse-biasing (orange background), the V_{OC} and *FF* of the cell with Al_2O_3 back-side passivation dropped significantly. In contrast, the cell with SiO_2 back-side passivation was almost unaffected by the reverse bias voltage of -6.7 V, even when applied for ~2 h (see Fig. 2b).

After the degradation by reverse-biasing, the IBC solar cell with Al_2O_3 back-side passivation regenerates already during the IV measurements under STC (see Fig. 2a). In order to further investigate this regeneration effect, dedicated measurements were performed. First, cells with SiO_2 and Al_2O_3 passivation were reverse biased for 10 s up to 33 h and the cell parameters were measured afterwards as fast as possible (which took about 1 to 3 min, cf. Fig. 2). It was found that the cell with Al_2O_3 passivation degrades continuously with time, i.e. the conversion efficiency was reduced by about 1 $\%_{abs}$ within 1 min and about 2 $\%_{abs}$ within 33 h of reverse bias (see Fig. 3a). Note that not the best cell but one with a high V_{OC} and *FF* was chosen (cf. Fig. 2a), so the initial efficiency was only 21.6 %. In contrast, the SiO_2 passivation turned out to be quite stable. The results indicate an efficiency loss of about 0.4 $\%_{abs}$ after 33 h of reverse bias, but such small changes are close to the measurement uncertainty as can be seen by the scattering of data in Fig. 2.

After degradation for 20 h under reverse bias, the regeneration of the cell with Al_2O_3 passivation was investigated under standard testing conditions (STC: 25 °C, 1 sun illumination) and at elevated temperatures on a hotplate (see Fig. 3b). The regeneration at STC was found to be quite slow, whereas at 100 °C (without illumination), a significant improvement was observed already within a couple of minutes. At 200 °C, the cell performance was almost fully recovered within only one minute. This regeneration behavior was fitted by a stretched exponential function

$$\eta = \eta_{\min} + \left(\eta_{\max} - \eta_{\min}\right) \cdot \left(1 - \exp\left(-\left(c \cdot t\right)^{\beta}\right)\right) \quad (1)$$

with the degraded efficiency η_{min}, the initial efficiency η_{max}, the exponential factor c, and the stretching exponent β.

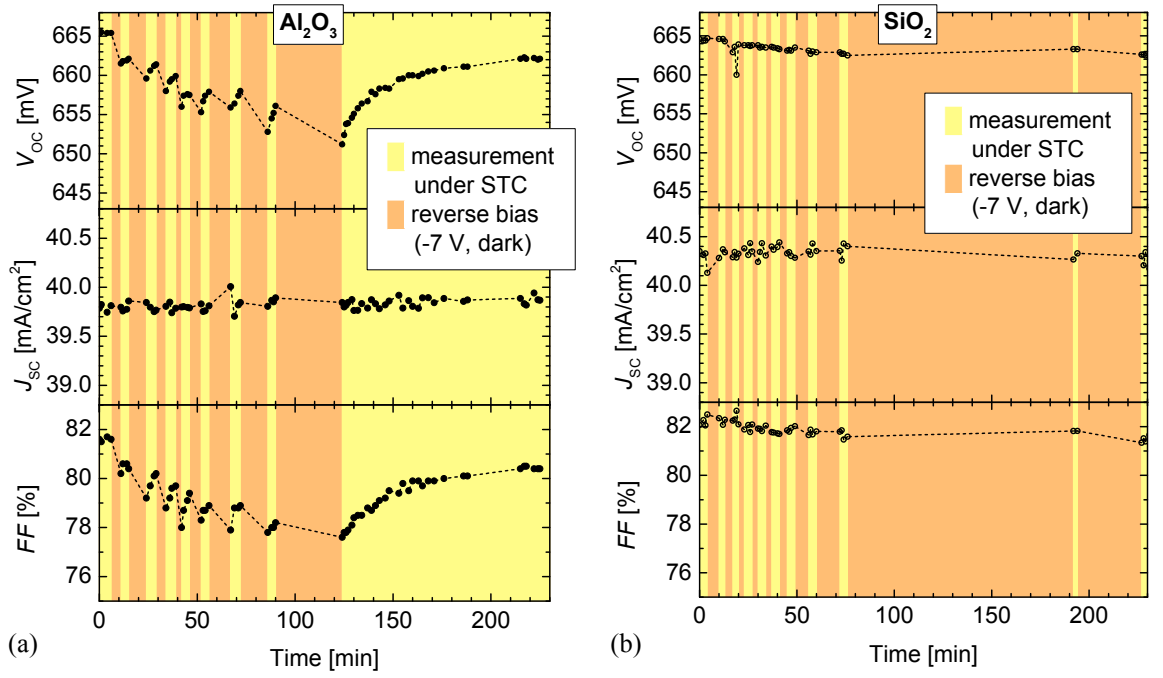

Fig. 2. Transient behaviour of the solar cell parameters during alternating conditions: reverse bias in the dark and IV measurement under standard testing conditions (STC). Dotted lines are just a guide to the eye.

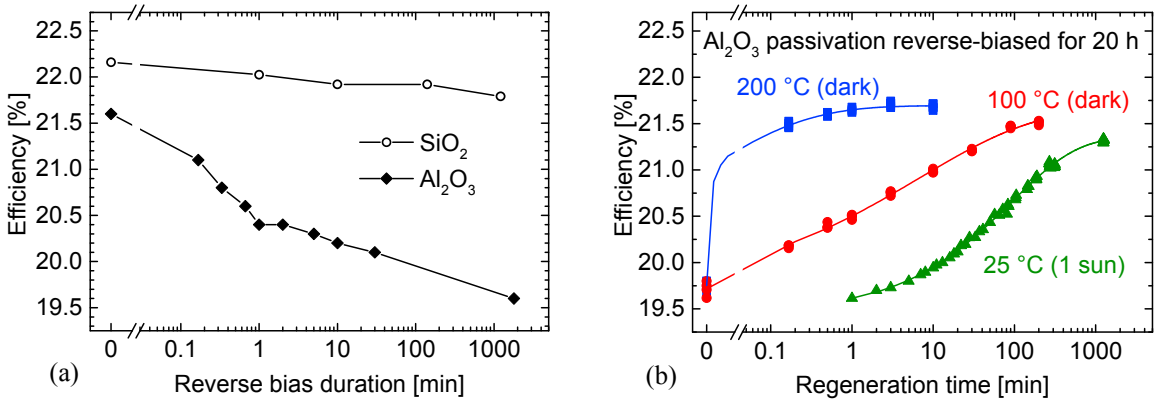

Fig. 3. Degradation (a) and regeneration (b) of the conversion efficiency of the IBC solar cell with SiO_2 or Al_2O_3 back-side passivation. The degradation was performed by reverse-biasing the cells at -6.7 V at room temperature. The regeneration was tested under STC (25 °C, 1 sun illumination) and at elevated temperature on a hotplate in the dark. Before the regeneration processes, the cell was degraded for 20 hours. Lines in (b) represent best fits with the stretched exponential function.

4. Discussion

In a former study on very similar solar cells, the degradation after reverse breakdown was related to an increase in recombination current density pre-factor with ideality factor of two (J_{02}) [12], i.e. an additional recombination of charge carriers in the space charge region. In principle, this could be a recombination localized within the silicon bulk where the emitter and BSF are in direct contact to each other, but there are two clear indications that the

degradation is not a bulk effect. Firstly, the cells with SiO_2 passivation were fabricated from the same silicon crystal and were doped identically, but do not show the strong degradation. Secondly, the regeneration at very low temperatures (≤ 100 °C) can hardly be explained by a bulk effect. As a consequence, the recombination occurs most probably where the p^+n^+ junction touches the surface.

The comparison of cells with different back-side layers is a clear indication, that the degradation of the cell performance is related to the Al_2O_3 passivation. Obviously, the reverse-bias voltage (or current) somehow affects the Al_2O_3 passivation quality, at least at the p^+n^+ junction. The passivation quality of Al_2O_3 is strongly based on negative charges. There are many different types of charges like fixed charges far away from the band gap of silicon, interface trap charges, etc. [14]. At least some of them can be discharged e.g. by an external voltage stress (charge trapping and detrapping) [15-17]. A reverse bias of the IBC solar cells results in a strong electric field within the passivation layer above the p^+n^+ junction that could cause a reversal of interface trap charges. This would lead to a decrease in passivation quality and hence an increase in J_{02}. In contrast, the SiO_2 passivation is mainly based on a low interface defect density and charges play only a minor role in the passivation quality, which would explain the difference to Al_2O_3.

Unfortunately, it is hard to distinguish experimentally between the influence of the interface defect density and the influence of the field effect due to charges, because the degradation due to reverse breakdown occurs only at the p^+n^+ junction and cannot be induced on a larger area for lifetime investigations. However, the regeneration behavior of the degraded Al_2O_3 passivation layer could reveal indications on the involved mechanisms. For example, Al_2O_3 layers have to be thermally activated to achieve a good surface passivation, but this activation typically starts at 200 to 300 °C for plasma-assisted as well as thermal atomic layer deposition processes [18]. Consequently, the regeneration mechanism observed for the IBC solar cells (Fig. 3) is probably different to the initial activation as it occurs at much lower temperatures. Nevertheless, the thermal activation of Al_2O_3 layers was fitted by a stretched exponential function [19] which is also applicable to the regeneration process of the Al_2O_3 passivation after reverse bias (cf. Fig. 3b).

There are also other treatments that damage the Al_2O_3 passivation but can be annealed at lower temperatures. For example, the radiation with an electron beam that can occur during evaporation of metals, usually damages passivation layers. This e-beam damage typically disappears after a thermal annealing at around 200 °C. However, the mechanism must be different to the reverse-bias degradation as SiO_2 passivation layers are also affected by the e-beam damage (cf. [20]).

5. Conclusions

Simplifications of the fabrication process for interdigitated back-contact (IBC) solar cells often result in the formation of p^+n^+ junctions if emitter and back-surface field are in direct contact to each other. This leads to a controlled breakdown at a low voltage under reverse bias, which is in principle an advantage for module integration. However, the reverse breakdown can cause a severe degradation of the cell performance, most probably due to a loss of passivation quality at the p^+n^+ junction at the back side. Al_2O_3 seems to be a bad choice for the back-side passivation as it is strongly affected by the reverse breakdown. In contrast, SiO_2 offers a quite stable passivation. Consequently, it is advisable to take special care of the back-side passivation layer if the IBC solar cells show a reverse breakdown. Other passivation layers than Al_2O_3 and SiO_2 were not yet investigated but might be affected as well. Furthermore, this topic could arise when dealing with IBC solar cells with passivating contacts or hetero junctions depending on the fabrication processes.

Acknowledgements

The authors want to thank Sonja Seitz, Andreas Lösel, Felix Schätzle, Antonio Leimenstoll, Karin Zimmermann, Astrid Seiler, Nadine Brändlin and Elisabeth Schäffer for sample processing, measurements, and technical support as well as the German Federal Ministry for Economic Affairs and Energy (contract number 0325292 „ForTeS“) and the European Union’s Seventh Programme (Grant No. 608498 “HERCULES”) for funding.

References

[1] D.D. Smith, P. Cousins, S. Westerberg, R. De Jesus-Tabajonda, G. Aniero, and Y.-C. Shen, Towards the Practical Limits of Silicon Solar Cells, *IEEE Journal of Photovoltaics* **4** (2014) 1465-1469.

[2] K. Yoshikawa, H. Kawasaki, W. Yoshida, T. Irie, K. Konishi, K. Nakano, T. Uto, D. Adachi, M. Kanematsu, H. Uzu, and K. Yamamoto, Silicon heterojunction solar cell with interdigitated back contacts for a photoconversion efficiency over 26%, *Nature Energy* **2** (2017) 17032.

[3] R.A. Sinton, and R.M. Swanson, Simplified backside-contact solar cells, *IEEE Transactions on Electron Devices* **37** (1990) 348-52.

[4] A. Halm, V.D. Mihailetchi, G. Galbiati, L.J. Koduvelikulathu, R. Roescu, C. Comparotto, R. Kopecek, K. Peter, and J. Libal, The Zebra Cell Concept - Large Area n-type Interdigitated Back Contact Solar Cells and One-Cell Modules Fabricated Using Standard Industrial Processing Equipment, in Proceedings of the *27th European PV Solar Energy Conference*, Frankfurt, 2012, pp. 567-570.

[5] M. Dahlinger, K. Carstens, E. Hoffmann, R. Zapf-Gottwick, and J.H. Werner, 23.2% laser processed back contact solar cell: fabrication, characterization and modeling, *Progress in Photovoltaics: Research and Applications* **25** (2017) 192-200.

[6] R. Keding, D. Stuwe, M. Kamp, C. Reichel, A. Wolf, R. Woehl, D. Borchert, H. Reinecke, and D. Biro, Co-Diffused Back-Contact Back-Junction Silicon Solar Cells without Gap Regions, *IEEE Journal of Photovoltaics* **3** (2013) 1236-1242.

[7] R. Müller, J. Schrof, C. Reichel, J. Benick, and M. Hermle, Back-junction back-contact n-type silicon solar cell with diffused boron emitter locally blocked by implanted phosphorus, *Applied Physics Letters* **105** (2014) 103503.

[8] J.D. Huyeng, R. Efinger, A. Spribille, R. Keding, A. Wolf, O. Doll, F. Clement, and D. Biro, Co-Diffused Back-Contact Back-Junction Silicon Solar Cells with a Novel Screen-Printed Boron-Doping Paste, in Proceedings of the *32nd EUPVSEC*, 2016, pp. 575-579.

[9] U. Römer, R. Peibst, T. Ohrdes, Y. Larionova, N.P. Harder, R. Brendel, A. Grohe, D. Stichtenoth, T. Wutherich, C. Schöllhorn, H.J. Krokoszinski, and J. Graff, Counterdoping with patterned ion implantation, in Proceedings of the *39th IEEE PVSC*, 2013, pp. 1280-1284.

[10] S. Gloger, A. Herguth, J. Engelhardt, G. Hahn, and B. Terheiden, A 3-in-1 doping process for interdigitated back contact solar cells exploiting the understanding of co-diffused dopant profiles by use of PECVD borosilicate glass in a phosphorus diffusion, *Progress in Photovoltaics: Research and Applications* **24** (2016) 955-967.

[11] G. Scardera, D. Inns, G. Wang, S. Dugan, J. Dee, T. Dang, K. Bendimerad, F. Lemmi, and H. Antoniadis, All-screen-printed Dopant Paste Interdigitated Back Contact Solar Cell, *Energy Procedia* **77** (2015) 271-278.

[12] R. Müller, C. Reichel, J. Schrof, M. Padilla, M. Selinger, I. Geisemeyer, J. Benick, and M. Hermle, Analysis of n-type IBC solar cells with diffused boron emitter locally blocked by implanted phosphorus, *Solar Energy Materials & Solar Cells* **142** (2015) 54-59.

[13] D.D. Smith, P.J. Cousins, A. Masad, S. Westerberg, M. Defensor, R. Ilaw, T. Dennis, N. Bergstrom, A. Leygo, X. Zhu, B. Meyers, B. Bourne, M. Shields, and R. Doug, SunPower's Maxeon Gen III solar cell: High Efficiency and Energy Yield, in Proceedings of the *39th IEEE Photovoltaic Specialists Conference*, Tampa, USA, 2013, pp. 908-913.

[14] S.M. Sze, Physics of Semiconductor Devices (*John Wiley & Sons, Inc.*, New York, 1981).

[15] J.A. Töfflinger, A. Laades, L. Korte, C. Leendertz, L.M. Montañez, U. Stürzebecher, H.-P. Sperlich, and B. Rech, PECVD-AlOx/SiNx passivation stacks on wet chemically oxidized silicon: Constant voltage stress investigations of charge dynamics and interface defect states, *Solar Energy Materials & Solar Cells* **135** (2014) 49-56.

[16] P.M. Jordan, D.K. Simon, T. Mikolajick, and I. Dirnstorfer, Trapped charge densities in Al2O3-based silicon surface passivation layers, *Journal of Applied Physics* **119** (2016) 215306.

[17] D. Suh, and W.S. Liang, Electrical properties of atomic layer deposited Al2O3 with anneal temperature for surface passivation *Thin Solid Films* **539** (2013) 309-316.

[18] A. Richter, J. Benick, M. Hermle, and S.W. Glunz, Reaction kinetics during the thermal activation of the silicon surface passivation with atomic layer deposited Al_2O_3, *Applied Physics Letters* **104** (2014) 061606.

[19] S. Kühnhold-Pospischil, P. Saint-Cast, A. Richter, and M. Hofmann, Activation energy of negative fixed charges in thermal ALD Al2O3, *Applied Physics Letters* **109** (2016) 061602.

[20] A.W. Blakers, M.A. Green, and T. Szpitalak, Surface damage caused by electron-beam metallization of high open-circuit voltage solar cells, *IEEE Electron Device Letters* **5** (1984) 246-247.